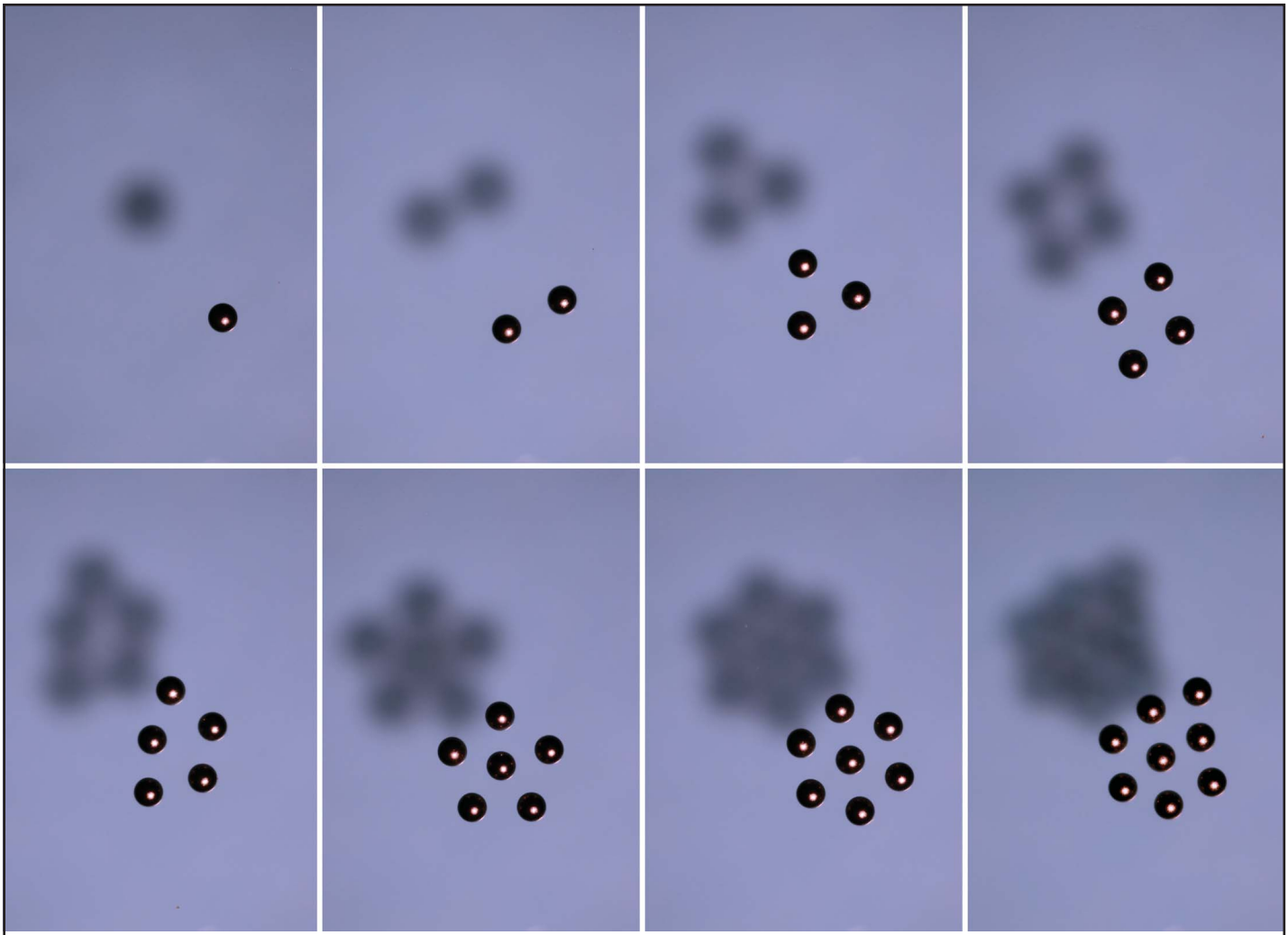

Highlighting research from GRASP, Department of Physics, University of Liège, Belgium.

Title: Self-assembled magnetocapillary swimmers

When identical soft ferromagnetic particles are placed on a liquid-air interface where a vertical magnetic field is applied, the balance of capillary attraction and magnetic repulsion creates a self-assembly. These structures are then perturbed by an oscillating horizontal field, resulting in a locomotion at low Reynolds number of the particle system. This tricky experiment opens new perspectives in soft matter since both capillary and magnetic interactions can be rescaled to small scales.

As featured in:

See N. Vandewalle *et al.*, *Soft Matter*, 2013, **9**, 2420.

RSC Publishing

www.rsc.org/softmatter

Registered Charity Number 207890

Soft Matter

RSC Publishing

PAPER

Self-assembled magnetocapillary swimmers†

Cite this: *Soft Matter*, 2013, **9**, 2420

G. Lumay,[a] N. Obara,[ab] F. Weyer[a] and N. Vandewalle*[a]

Received 30th August 2012
Accepted 17th December 2012

DOI: 10.1039/c2sm27598h

www.rsc.org/softmatter

When particles are suspended at air–water interfaces in the presence of a vertical magnetic field, dipole–dipole repulsion competes with capillary attraction such that 2d ordered structures self-assemble. By adding a horizontal and oscillating magnetic field, periodic deformations of the assembly are induced. We show herein that pulsating particle arrangements start to swim at low Reynolds number. We identify the physical mechanisms and geometrical ingredients behind this cooperative locomotion. These physical mechanisms can be exploited to much smaller scales, offering the possibility to create artificial and versatile microscopic swimmers.

1 Introduction

The attractive interaction between small floating bodies originates from the deformations of the fluid interface around the particles. This phenomenon is called the "Cheerios effect",[1] a reference to clumping of cereals in a breakfast bowl. Experimental studies evidenced complex mechanisms and non-obvious patterns even for a low number of floating bodies.[2,3] Despite being a subject with tricky experiments, the fundamental and technological implications of the Cheerios effect are far from frivolous. Indeed, extensive research demonstrated that the self-assembly of small-scale structures can be achieved along liquid interfaces, opening ways to much simplified manufacturing processes of micro-electromechanical systems.[4,5]

Self-assembly is directed towards well ordered structures when magnetic particles are placed at liquid interfaces.[6] This magnetic Cheerios effect[7] is illustrated in Fig. 1. Let us consider the case of N submillimeter soft ferromagnetic beads placed at the air–water interface. Floating is ensured by the partial wetting of the dense spherical objects, creating a meniscus with a typical size given by the capillary length $\lambda = \sqrt{\gamma/\rho g}$ where γ is the surface tension, ρ is the liquid density and g is the gravity acceleration. For air–water interfaces, $\lambda \approx 2.5$ mm, which is much larger than the largest bead diameter used in our work ($D = 500$ μm). A vertical field B_z induces repulsive dipole–dipole interactions between magnetized particles. As illustrated in Fig. 1, the competition between long-range capillary attraction and short-range magnetic repulsion defines equilibrium interdistances for the particles along the liquid interface.[7] In Fig. 1, the pictures of the various configurations are obtained for an increasing number of small floating objects in a constant vertical magnetic field. Configurations display symmetrical features, as expected from isotropic interactions:[6] particles tend indeed to be located at the vertices of 2d crystals. It is also possible to downscale this ordering since both magnetic and capillary interactions[7] are still playing a role at the micrometer scale. By adjusting B_z, the particle interdistance is tuned.[7] Such a field-controlled process is fully reversible as long as bead–bead contacts, occurring at low B_z values, are avoided. One should remark that for a fixed B_z value, the average nearest neighbor distance decreases with N. This is due to curvature effects at the scale of the raft.[8]

In this paper, we investigate the dynamics of self-assembled ferromagnetic beads submitted to a periodic forcing. A horizontal and oscillating magnetic field $B_x = B_{0x}\sin(2\pi ft)$ is applied. As a consequence, additional dipole–dipole interactions deform the assembly along both x (attraction) and y

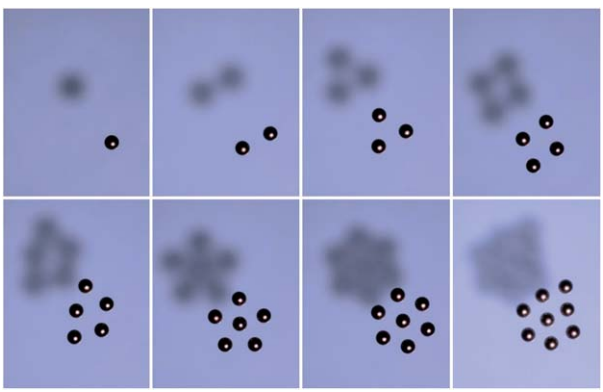

Fig. 1 Series of top images of floating beads (diameter $D = 500$ μm, $N = 1$ to 8) when the vertical field is switched on ($B_z = 25$ G). The horizontal field is off. Small "crystals" are obtained when a few beads are placed at the liquid–air interface. Lightning from above creates a shadow at the bottom of the container.

[a]*GRASP, Institut de Physique B5a, Sart Tilman, University of Liège, Belgium. E-mail: geoffroy.lumay@ulg.ac.be; Web: http://www.grasp-lab.org*

[b]*Department of Physics, Graduate School of Ochanomizu University, 2-1-1, Otsuka, Bunkyo-ku, Tokyo 112-8610, Japan. E-mail: nvandewalle@ulg.ac.be*

† Electronic supplementary information (ESI) available: Three movies[9–11] accompany the paper. See DOI: 10.1039/c2sm27598h

(repulsion) directions. Patterns are studied as a function of time.

2 Experimental setup

The experimental setup is illustrated in Fig. 2. A large Petri dish is filled with water. In some experiments, the viscosity of the liquid has been modified by considering glycerol–water mixtures which allows for a significant increase of η while the surface tension γ is slightly reduced. The liquid–air interface is placed at the center of biaxial Helmholtz coils. When a current i is applied in such coils, a uniform and vertical magnetic field B_z is obtained in the Petri dish. Magnetic fields up to 30 G have been considered. Oscillations of the horizontal field B_x are provided by a function generator and an amplifier. Chrome steel particles (selected alloy AISI 52100, $\rho_s = 7830$ kg m^{-3}) do not exhibit any hysteretic behavior in the range of field values used herein. As a result, one particle does not retain any residual magnetic moment once the field is removed. Prior to experiments, spheres are washed with acetone and thereafter dried in an oven. Two different bead diameters have been studied: $D = 400$ μm and $D = 500$ μm. Partial wetting ensures the floatation of the spheres. In most experiments, spheres are always separated from each other before relaxing the system. A high resolution CCD camera records images from top. Image analysis provides both position $\vec{r}_i$ and velocity $\vec{v}_i$ for each bead i as a function of time t.

Two pictures of a triplet are given in Fig. 3. The liquid interface is curved since the system is placed in a test tube instead of a Petri dish, in order to trap the triplet in the center of the system. The side view of the triplet shows us that a large part of the beads (roughly 80%) is immersed. In order to avoid any irreversible contact between pairs of neighboring particles, the amplitude of the oscillating field is always limited, following the empirical condition $B_{0x} < B_z/2$. The energy injected into the system is mainly dissipated due to viscous effects. A time τ_v, characterizing the viscous damping of any bead motion, is given by $\tau_v = \rho_s D^2/18\eta \approx 0.07$ s, where ρ_s is the bead density and η is the water viscosity (10^{-3} Pa s). The response of the self-assembly to periodic forcing is therefore dominated by viscous effects when the frequency f is below $f_v = 1/\tau_v \approx 14$ Hz. The results presented herein are obtained for a fixed frequency $f = 1.5$ Hz. Other values of the forcing frequency have been investigated below f_v and results remain qualitatively unchanged.

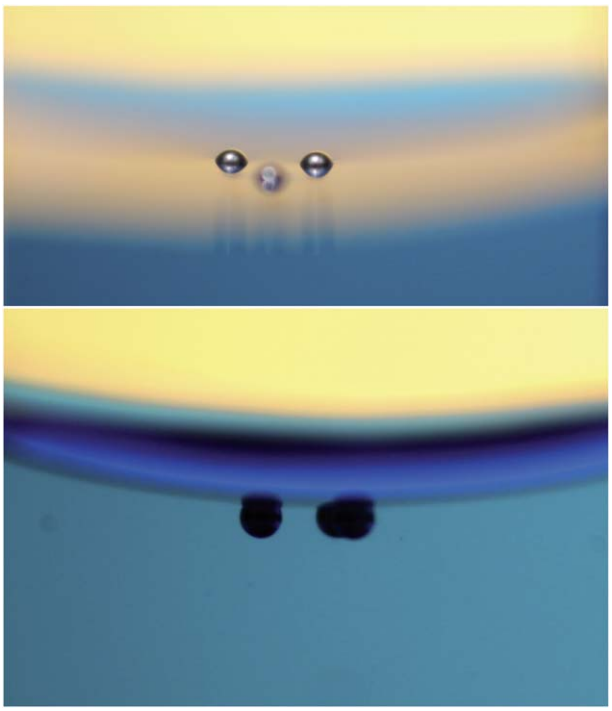

Fig. 3 (Top) Picture of a triplet in a test tube ($D = 500$ μm, $B_z = 25$ G). The whole air–water interface is curved such that the triplet is trapped in the center of the tube. The deformation of the interface near the spherical caps can be seen. (Down) Side view of the same triplet in a test tube. About 80% of the particle volume is immersed.

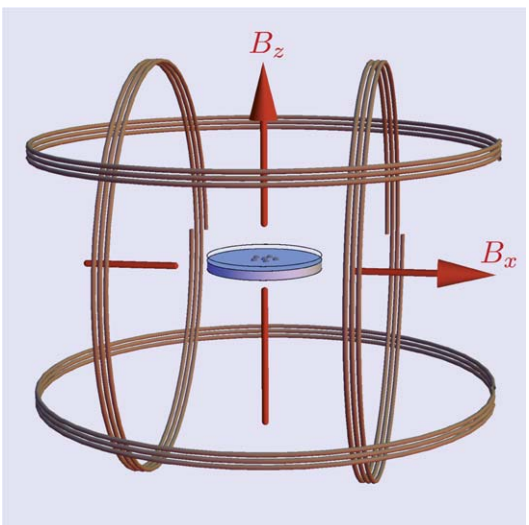

Fig. 2 Sketch of our experimental setup. Soft ferromagnetic particles are self-assembling at the water–air interface in a Petri dish. The latter is placed at the center of biaxial Helmholtz coils. A vertical and constant magnetic field B_z is applied through the system. An oscillating horizontal field B_x excites the self-assembled structures at frequency f.

One should stress that our experimental setup has 7 relevant parameters: N, D, η, γ, f, B_{0x} and B_z. Each parameter has been considered for testing the robustness of our findings described below. In the present article, we will focus on the magnetic fields B_{0x} and B_z as well as the size N of the particle clusters. Different viscosities were also considered, as shown at the end of this paper. For each set of parameters, 200 pulsation periods are recorded, corresponding to about 2000 images before numerical treatment. This procedure has been repeated many times (typically 10–20 times) in order to collect a large set of data.

3 Experimental results

As expected, the periodic forcing along the x axis drives the assembly into pulsating modes. The oscillating dipole–dipole interactions induce non-trivial collective motions of the

particles. In fact, when the strength of the oscillating field B_x is small, particles circle around their equilibrium positions. By increasing the strength of the oscillating field, *i.e.* by increasing B_{0x}, periodic trajectories with a translational component are triggered. Fig. 4a–d illustrate such trajectories of the particles over ten periods, obtained by image analysis. Four different assemblies are presented ($N = 3, 4, 5, 6$) for high B_{0x} values. The typical amplitude of the bead displacements over one period corresponds to $\delta \approx D/10$, while the average interdistance $\langle r_{ij} \rangle$ between two nearest neighboring beads i and j is typically in between $1.5D$ and $2.8D$ depending on B_z. An oscillating pair of particles ($N = 2$) tends to be aligned with respect to the horizontal field, but the center of mass remains immobile. However, triplets of particles ($N = 3$) are moving along the (x, y) plane, as shown in Fig. 4a. A significant displacement over ten periods is seen along some diagonal direction.[9] By changing the horizontal field orientation (by switching the oscillation between y and x axes for example), the swimmer motion is modified indicating that preferential orientations exist with respect to the horizontal field axis.[10] Fig. 4b presents a quadruplet ($N = 4$), which fluctuates around a nearly fixed position, even individual particles are dancing cooperatively. This diamond configuration is in fact a poor swimmer. As shown in Fig. 4c, the $N = 5$ assembly exhibits large deformations, and a net propulsion is observed along specific diagonal directions. In Fig. 4d, the locomotion of the $N = 6$ pentagonal structure is seen. Over long runs (165 periods are shown in Fig. 4e), particle trajectories are decorated with loops. Although propulsion of the group of particles is seen along the x axis, intermittent events take place due to some rotational reorganization of the structure.[11] When the number of components increases, the trajectories become more and more complex. For larger particle assemblies, the situation becomes delicate, because the mean distance between nearest neighboring beads decreases such that irreversible particle–particle contact could occur. Only poor swimmers have been obtained for $N > 6$.

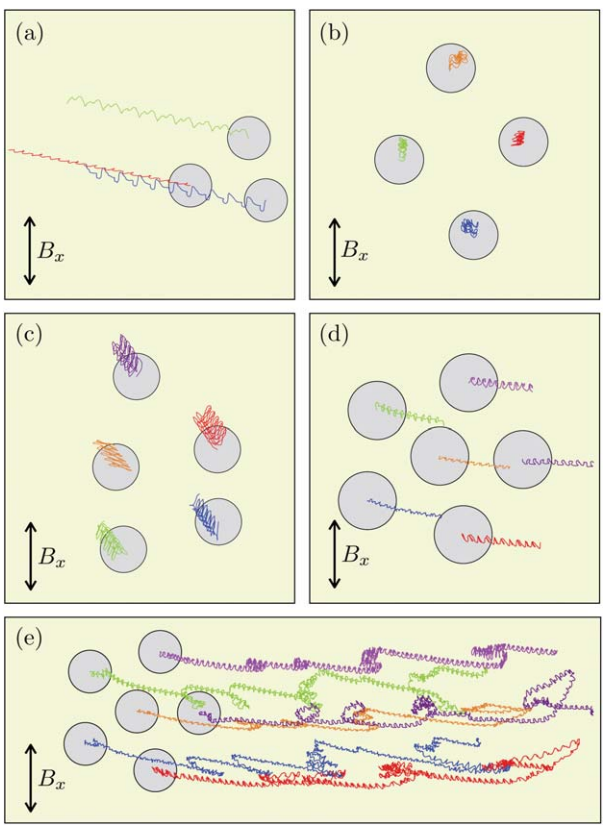

Fig. 4 Typical bead trajectories for $N = 3, 4, 5, 6$ self-assemblies during ten periods (a–d) and 165 periods (e). The orientation of the oscillating magnetic field B_x is indicated. The beads are drawn in grey in order to emphasize the scale of the plots ($D = 500$ μm). (a) The $N = 3$ group of magnetic particles is an efficient swimmer along an oblique direction. (b) The center of mass of an $N = 4$ diamond assembly is fluctuating around its initial position. (c) The $N = 5$ assembly is swimming. (d and e) The $N = 6$ assembly shows intermittent behavior seen in the case of long runs: translation stages separated by rotational events.

Efficient synthetic locomotion is induced by a strong oscillating field B_x for specific N values. Average speeds of the center of mass up to $v = 0.5D/T$ (in bead diameter per period) have been reached in our experiments. The fundamental question concerns the physical mechanism behind this cooperative locomotion.

Earlier studies[12–14] considered magnetically driven dynamic systems. Although field orientations are different and particle contacts are allowed, the case of several magnetic grains placed at the liquid–air interface and submitted to an oscillating field exhibits moving self-assembled structures as well. However, this particular locomotion is completely different to our system because it is induced by the capillary waves generated by the periodic displacement of particle aggregates along the interface. The capillary wavelength in our experiment is $\Lambda = (2\pi\gamma/\rho f^2)^{1/3} \approx 6$ cm, *i.e.* much larger than the particle systems. Moreover, we measured the meniscus profile around particle clusters using the method of optical refracted image correlations developed by Moisy *et al.*[15] From those experiments, we observed that the amplitude of the water profile along the z axis was always below 10 μm. If capillary waves are generated by the bead motion, their amplitudes are extremely low and a weak interaction with the assembly is therefore expected. The origin of the synthetic cooperative locomotion reported herein is therefore based on a different mechanism.

Since the amplitude of the oscillations is $\delta < D$, the Reynolds number can be estimated by taking $\mathrm{Re} = \rho\delta D 2\pi f/\eta$. In our experiments, typical values of Re are in between 0.01 and 0.2. The locomotion of self-assembling particles is therefore dominated by viscous forces. Low Reynolds swimming is a non-trivial phenomenon. Different physical ingredients could play a role. It is known to originate from the association of hydrodynamic coupling and a non-reciprocal deformation of the swimming body.[16–18] The hydrodynamic coupling depends on the relative velocities of all pairs of particles in the system. Nonreciprocal motion is only possible for $N > 2$. The basic unit, able to generate a non-reciprocal motion, is a triplet, in agreement with our experimental results.

We have investigated how non-reciprocal triplet deformations take place. Without horizontal excitation, the triplet shape is a static regular triangle like the one shown in Fig. 1. When the oscillating horizontal field is switched on, the triplet deforms with a frequency $2f$ since the periodic dipole–dipole interaction

scales as $B_x^2 = B_{0x}^2 \sin^2(2\pi ft)$. As expected for nonlinear interactions, several vibration modes of the triplet can be excited depending on the initial conditions. After a few periods, the dynamical system is locked into a specific mode. Fig. 5a and b present the time evolution of the particle separations r_{12}, r_{23} and r_{13} over three periods for the same set of parameters but for different initial conditions. The corresponding trajectories over 10 periods are also illustrated at the right of each plot. Two different pulsating modes have been selected. One distance exhibits large oscillations compared to others. This corresponds to a pair of particles nearly aligned along the oscillating field. The oscillations at frequency $2f$ are superimposed to f-periodic oscillations. Indeed, the magneto-capillary system could be seen as a set of coupled parametric oscillators.[22] When excited at frequency $2f$, these oscillators exhibit parametric resonances like period doubling, *i.e.* oscillations at frequency f. Multiple modes also coexist, as illustrated by Fig. 5a and b. Although the distances are oscillating around the similar static equilibrium ones, pulsating modes are drastically different: the phase shift between the curves of (a) is weak, while a significant phase shift is clearly observed for (b). The latter is a clear signature of non-reciprocal motion. The study of their respective motions reveals that the triplet (a) is a poor swimmer while (b) is an efficient one. It should be remarked that it is possible to switch from a mode to another one by switching off the field for a short period in order to 'reset' the system[10] or by changing the direction of the horizontal field. Actually, a specific pulsating mode cannot be selected in our experimental procedure. This is outside the scope of the present paper but remains a clear motivation for future works. The plot of Fig. 5c, obtained for a higher B_z value, shows larger average distances than previous cases and more pronounced period doubling components, *i.e.* large periodic patterns at frequency f. It appears that this pulsating swimmer is less efficient. The field B_z has indeed an effect on the locomotion, as we will see below.

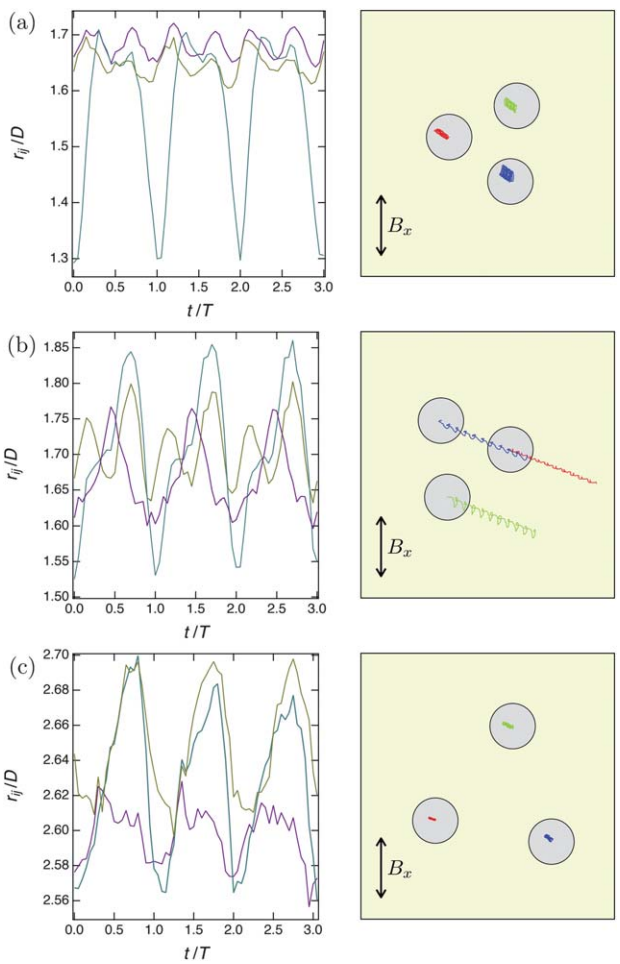

Fig. 5 (a) The distances r_{ij} between particles in a pulsating triplet for $B_{0x} = 5$ G and $B_z = 14$ G. Three periods are shown. This triplet is a poor swimmer, as seen in the corresponding trajectories over 10 periods. Different bead trajectories are colored in red, blue and green. Interdistances (left plot) are emphasized in medium colors: purple (distance between red and blue), teal (distance between blue and green) and olive (distance between red and green). (b) Same plot for the same set of parameters but for different initial conditions. This triplet is an excellent swimmer as seen in the corresponding trajectories in the right plot. (c) The triplet distances as a function of time, for $B_{0x} = 5$ G and $B_z = 25$ G. The triplet is a poor swimmer since larger interdistances imply weak hydrodynamic interactions.

Fig. 6 presents the speeds recorded for various triplets as a function of B_z, keeping $B_{0x} = 5$ G constant. For a fixed set of (B_{0x}, B_z) parameters, different propulsion modes with different associated speeds are seen. These modes are excited by starting from different initial conditions. As shown in a previous work,[7] the equilibrium distance between beads increases monotoneously with B_z. The driving force of low Reynolds swimming is the hydrodynamics interaction between moving particles. As discussed in the next section, the later force scales as D/r_{ij}, such that low B_z values imply higher speeds as seen in Fig. 6.

The viscosity η of the liquid affects also the swimming speed, as shown in Fig. 6. Results are shown for a glycerol–water

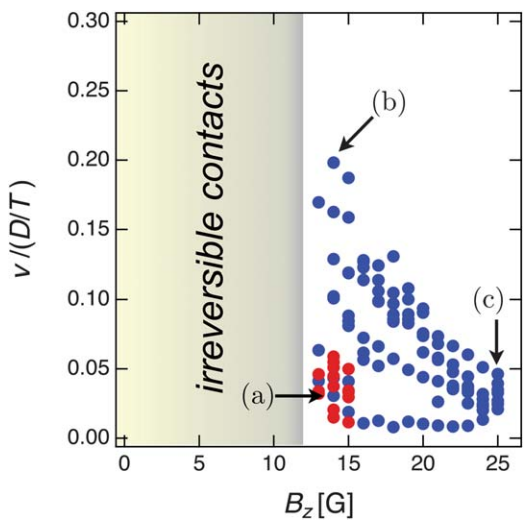

Fig. 6 Swimming speed v as a function of the vertical magnetic field B_z when $B_{0x} = 5$ G is kept constant. Different blue data points correspond to different modes obtained from different initial conditions. Three pulsation modes illustrated in Fig. 5a–c are indicated by arrows (a), (b) and (c). The red dots show similar data obtained at the surface of a water–glycerol mixture (75–25%) being 2.5 times more viscous than pure water. The swimming speeds are reduced by the same factor 2.5.

mixture (η being 2.5 times higher than viscosity of water). The swimming speeds are reduced by around a factor 2.5, as expected if one considers that hydrodynamic coupling is the major physical ingredient for locomotion.[21] Higher viscosities (ten times the viscosity of water) have been tested but locomotion was so slow that we were unable to measure precisely the resulting speed.

4 Discussion

In the previous section, we have shown in experiments that the vibrations of self-assembled magnetic particles can be exploited to induce low Reynolds locomotion. The relevant question concerns the design of an optimal swimmer. What are the parameters for controlling the speed of magnetocapillary swimmers?

The major physical mechanism of swimming at low Reynolds number is the hydrodynamic coupling between the different components of the swimmer, *i.e.* between the particles. In the Stokes regime, an expression of this coupling has been derived for identical spheres[19] and is strongly dependent on the particle interdistances r_{ij}. One has

$$\vec{F}_h = \frac{9\pi}{8}\eta D^2 \sum_{j\neq i} \frac{(\vec{v}_j\cdot\vec{n}_{ij})\vec{n}_{ij} + \vec{v}_j}{r_{ij}}, \quad (1)$$

being the force acting on particle i due to the motion of the other particles $j \neq i$ in the fluid. The unit vectors are given by $\vec{n}_{ij} = (\vec{r}_j - \vec{r}_i)/r_{ij}$. The main parameters of the hydrodynamic coupling are (i) the relative distances r_{ij} between particles, (ii) the particle velocities $\vec{v}_j$, and (iii) the viscosity η.

A strong coupling is expected when particles are close together. This distance is tuned by the vertical field B_z since the magnetic repulsion counterbalanced by the capillary attraction gives an equilibrium distance

$$r^* \approx \alpha B_z, \quad (2)$$

that we demonstrated in a recent work.[7] The coefficient α depends on both magnetic and wetting properties of the beads. This linear behavior holds above the collapse, *i.e.* for $B_z > D/\alpha$. From above arguments, one can understand that the optimal swimming conditions correspond to low B_z values, just above irreversible contact, as shown in Fig. 6.

As demonstrated by Najafi and Golestanian[20] for a system of three particles, the hydrodynamic coupling should be associated with nonreciprocal motion for providing a thrust to the particle system. Nonreciprocal motion corresponds to a cycle in the configuration space of the particle system. Golestanian and Ajdari[21] described the nonreciprocal motion in terms of phase shifts for particle oscillations. In the present system, the particle motion is provided by the horizontal magnetic field oscillations $B_x = B_{0x}\sin(\omega t)$, through dipole–dipole interactions. One has the force

$$\vec{F}_x = \frac{\mu_0}{4\pi}\frac{\pi^2 D^6 \chi^2 {B_x}^2}{36} \sum_{j\neq i} \frac{\vec{n}_{ij} - 5\left(\vec{e}_x\cdot\vec{n}_{ij}\right)^2\vec{n}_{ij} + 2\left(\vec{e}_x\cdot\vec{n}_{ij}\right)\vec{e}_x}{{r_{ij}}^4} \quad (3)$$

acting on particle i from dipoles of particles $j \neq i$. The parameter χ is the magnetic susceptibility of the beads. The force F_x is nonlinear and highly anisotropic. Due to the nonlinearities of eqn (3), one expects the coexistence of several pulsating modes, as recorded in our experiment (see Fig. 5 and 6). It should be noted that a single dipole in an oscillating field[22] exhibits already complex dynamics and a cascade of bifurcation. A deeper analysis of the nonlinear dynamics provided by magnetocapillary systems is therefore relevant, but still outside the scope of the present paper. As a function of the initial conditions and the amplitude of field oscillations, the system adopts a pulsating mode characterized by its own trajectory in the phase space. The pulsating motion of a triplet could be more or less nonreciprocal since different phase shifts between the oscillations of the system components have been observed for the same set of experimental conditions.

From both conditions (coupling and nonreciprocal motion), we deduce that the best conditions for swimming are when B_z is close to $2B_{0x}$. This is confirmed by the plot of Fig. 6. The ideal conditions for locomotion is therefore a compromise between both magnetic field strentghs.

For a fixed B_z value, the average interdistance between particles decreases with N due to the liquid–air interface curvature induced by the assembly. When the number of particle increases, the amplitude of oscillations should be more and more limited in order to avoid contacts. The result is a clear decrease of the maximum swimming speed of the assembly with N. Moreover, the complexity of the pulsating modes increases with N such that nonlinear trajectories are observed.

5 Conclusion

In summary, we have demonstrated that locomotion of self-assembled structures is possible thanks to the non-reciprocal vibrations of small rafts. The interplay of the geometry and the number of elements is as important as the physical parameter values. The most important feature of our system is that both self-assembling and periodic deformations can be rescaled to smaller sizes. Rich behaviors are expected when two or more swimmers start to interact, when the number of beads increases or when different bead sizes are considered.

Future efforts should be made in order to select pulsating modes and to control the motion of swimmers. This step will be achieved when a link can be established between pulsating modes and initial conditions. Numerical simulations represent a valuable approach for this task.

Acknowledgements

GL thanks FNRS for financial support. This work was also supported by the JSPS Institutional Program for Young Researcher Overseas Visits. This work is financially supported by the University of Liège (Grant FSRC-11/36).

References

1 D. Vella and L. Mahadevan, *Am. J. Phys.*, 2005, **73**, 817.

2 M. Berhanu and A. Kudrolli, *Phys. Rev. Lett.*, 2010, **105**, 098002.
3 M. J. Dalbe, D. Cosic, M. Berhanu and A. Kudrolli, *Phys. Rev. E: Stat., Nonlinear, Soft Matter Phys.*, 2011, **83**, 051403.
4 G. M. Whitesides and B. Grzybowski, *Science*, 2002, **295**, 2418.
5 J. A. Pelesko, *Self-assembly*, Chapmann & Hall, Boca Raton, 2007.
6 M. Golosovsky, Y. Saado and D. Davidov, *Appl. Phys. Lett.*, 1999, **75**, 4168.
7 N. Vandewalle, L. Clermont, D. Terwagne, S. Dorbolo, E. Mersch and G. Lumay, *Phys. Rev. E: Stat., Nonlinear, Soft Matter Phys.*, 2012, **85**, 041402.
8 D. Vella, P. D. Metcalfe and R. J. Whittaker, *J. Fluid Mech.*, 2006, **549**, 215.
9 Movie 1 – a triplet being an efficient swimmer. At the end of the movie, the field is switched off and the swimmer stops.
10 Movie 2 – a triplet is swimming. The horizontal field B_{0x} is switched off and the swimmer stops. The field is then switched on. The triplet locomotion resumes. Since another pulsating mode is selected, the direction of motion is changed.
11 Movie 3 – the motion of a swimming $N = 6$ self-assembly having a pentagonal shape. The movie emphasizes the complex intermittent behavior discussed in the main text.
12 A. Snezhko, M. Belkin, I. S. Aranson and W.-K. Kwok, *Phys. Rev. Lett.*, 2009, **102**, 118103.
13 A. Snezhko and I. S. Aranson, *Nat. Mater.*, 2011, **10**, 698.
14 R. Dreyfus, J. Baudry, M. L. Roper, M. Fermigier, H. A. Stone and J. Bibette, *Nature*, 2005, **437**, 862.
15 F. Moisy, M. Rabaud and K. Salsac, *Exp. Fluids*, 2009, **46**, 1021.
16 E. M. Purcell, *Am. J. Phys.*, 1977, **45**, 11.
17 E. Lauga and T. R. Powers, *Rep. Prog. Phys.*, 2009, **72**, 096601.
18 E. Lauga, *Soft Matter*, 2011, **7**, 3060.
19 L. D. Landau and E. M. Lifshitz, *Fluid Mechanics*, Butterworth-Heinemann, 2nd edn, 1987.
20 A. Najafi and R. Golestanian, *Phys. Rev. E: Stat., Nonlinear, Soft Matter Phys.*, 2004, **69**, 062901.
21 R. Golestanian and A. Ajdari, *Phys. Rev. E: Stat., Nonlinear, Soft Matter Phys.*, 2008, **77**, 036308.
22 H. Meissner and G. Schmidt, *Am J. Phys.*, 1986, **54**, 800.